An Overview of $B \to K^{(*)}\mu^+\mu^-$: What shall we expect?

Joaquim Matias
Universitat Autònoma de Barcelona

Paris

June 2, 2014

PLAN of the TALK

- Theoretical and experimental overview of the 4-body decay $B \to K^*(\to K\pi) l^+ l^-$ mode in terms of an optimal basis of CP conserving observables: $P_i^{(\prime)}$.
  Implications of BR of $B \to K^* \mu^+ \mu^-$ and $B \to K \mu^+ \mu^-$ on the analysis.
- Possible explanations for the observed tensions with the SM.
- A consistency test on data on $B \to K^* \mu^+ \mu^-$ for future analysis.
  A new relation between the zero of A_{FB} and the anomaly in P_5'.

Future ? ...

The angular distribution $\bar{\mathbf{B}}_\mathbf{d} \to \bar{\mathbf{K}}^{*\mathbf{0}}(\to \mathbf{K}^-\pi^+)\mathbf{l}^+\mathbf{l}^-$ with the K^{*0} on the mass shell. It is described by $\mathbf{s} = \mathbf{q^2}$ and three angles θ_ℓ, $\theta_\mathbf{K}$ and ϕ

$$\frac{d^4\Gamma(\bar{B}_d)}{dq^2\, d\cos\theta_\ell\, d\cos\theta_K\, d\phi} = \frac{9}{32\pi}\mathbf{J}(\mathbf{q^2}, \theta_\ell, \theta_K, \phi) = \frac{9}{32\pi}\sum_i J_i(q^2) f_i(\theta_\ell, \theta_K, \phi)$$

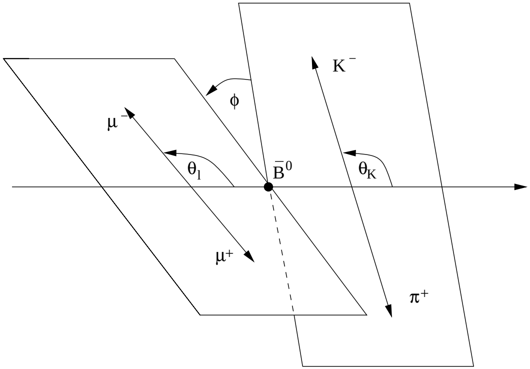

θ_ℓ: Angle of emission between $\bar{K}^{*0}$ and μ^- in di-lepton rest frame.
$\theta_\mathbf{K}$: Angle of emission between $\bar{K}^{*0}$ and K^- in di-meson rest frame.
ϕ: Angle between the two planes.

$\mathbf{q^2}$: dilepton invariant mass square.

Notice LHCb uses $\theta_\ell^{LHCb} = \pi - \theta_\ell^{us}$

Three regions in q^2:

- **large recoil for** K^*: $E_{K^*} \gg \Lambda_{QCD}$ or $4m_\ell^2 \le q^2 < 9$ GeV^2
- resonance region ($q^2 = m^2_{J/\Psi}, \ldots$) betwen $9 < q^2 < 14$ GeV^2.
- **low-recoil for** K^*: $E_{K^*} \sim \Lambda_{QCD}$ or $14 < q^2 \le (m_B - m_{K^*})^2$.

How to extract all the information from $B \to K^*(\to K\pi)\mu^+\mu^-$?

$\boxed{1}$ Use $J_k \to \mathrm{Re}(A_i^L A_j^L \pm A_i^R A_j^R)$ or $\mathrm{Im}(A_i^L A_j^L \pm A_i^R A_j^R)$

However $J_k \propto \xi_{\perp,\|}^2 \Rightarrow$ Theory uncertainty very large.

$\boxed{2}$ Use $S_i \to (J_i + \bar{J}_i)/(d\Gamma + d\bar{\Gamma})$ and $A_i \to (J_i - \bar{J}_i)/(d\Gamma + d\bar{\Gamma})$

However: - Sensitivity at LO to soft form factors $\xi_{\perp,\|}$ $\Downarrow$
- Scheme dependence when SFF are used $\Downarrow$ but not if pc are included $\Uparrow$
- Dependence on problematic form factor A_0 albeit m_ℓ suppressed $\Downarrow$
- m_ℓ dependence on β_ℓ but also m_ℓ terms. $\Uparrow$ $\Downarrow$

$\boxed{3}$ Use $P_k^{(\prime)} \to \mathrm{Re}\tilde{A}_i\tilde{A}_j/\sqrt{|\tilde{A}_i|^2|\tilde{A}_j|^2}$ (or Im) with $\tilde{A}_i \to A_i + \bar{A}_i$

$P_k^{CP} \to \mathrm{Re}\hat{A}_i\hat{A}_j/\sqrt{|\tilde{A}_i|^2|\tilde{A}_j|^2}$ (or Im) with $\hat{A}_i \to A_i - \bar{A}_i$

However: - Sensitivity **only** at NLO to soft form factors $\xi_{\perp,\|}$ $\Uparrow$
- **Marginal** scheme dependence when SFF are used $\Uparrow$ with or without pc.
- No dependence on problematic form factor A_0 $\Uparrow$
- Some observables identical for $m_\ell = e, \mu, \tau \Rightarrow$ excellent cross check . $\Uparrow$

P_i, P'_i defines an **Optimal Basis** of observables, a compromise between:

- *I. Excellent experimental accessibility and simplicity of the fit.*
- *II. Reduced FF dependence (in the large-recoil region:* $0.1 \leq q^2 \leq 8\ \mathrm{GeV}^2$).

Our proposal for **CP-conserving basis**:

$$\left\{\frac{\mathbf{d\Gamma}}{\mathbf{dq^2}}, \mathbf{A_{FB}}, \mathbf{P_1}, \mathbf{P_2}, \mathbf{P_3}, \mathbf{P'_4}, \mathbf{P'_5}, \mathbf{P'_6}\right\} \text{ or } \mathbf{P_3} \leftrightarrow \mathbf{P'_8} \text{ and } \mathbf{A_{FB}} \leftrightarrow \mathbf{F_L}$$

where $P_1 = A_T^2$ [Kruger, J.M'05],
$P_2 = \frac{1}{2} A_T^{\mathrm{re}}, P_3 = -\frac{1}{2} A_T^{\mathrm{im}}$ [Becirevic, Schneider'12]
$P'_{4,5,6}$ [Descotes, JM, Ramon, Virto'13]).

The corresponding **CP-violating basis** ($J_i + \bar{J}_i \rightarrow J_i - \bar{J}_i$ in numerators):

$$\left\{\mathbf{A_{CP}}, \mathbf{A_{FB}^{CP}}, \mathbf{P_1^{CP}}, \mathbf{P_2^{CP}}, \mathbf{P_3^{CP}}, \mathbf{P_4^{\prime CP}}, \mathbf{P_5^{\prime CP}}, \mathbf{P_6^{\prime CP}}\right\} \text{ or } \mathbf{P_3^{CP}} \leftrightarrow \mathbf{P_8^{\prime CP}} \text{ and } \mathbf{A_{FB}^{CP}} \leftrightarrow \mathbf{F_L^{CP}}$$

Analysis of new LHCb data on $B \to K^* \mu^+ \mu^-$

Present bins: [0.1,2], [2,4.3], [4.3,8.68], [1,6], [14.18,16], [16,19] GeV^2.

Observable	Experiment	SM prediction	Pull
$\langle P_1\rangle_{[0.1,2]}$	$-0.19^{+0.40}_{-0.35}$	$0.007^{+0.043}_{-0.044}$	-0.5
$\langle P_1\rangle_{[2,4.3]}$	$-0.29^{+0.65}_{-0.46}$	$-0.051^{+0.046}_{-0.046}$	-0.4
$\langle P_1\rangle_{[4.3,8.68]}$	$0.36^{+0.30}_{-0.31}$	$-0.117^{+0.056}_{-0.052}$	$+1.5$
$\langle P_1\rangle_{[1,6]}$	$0.15^{+0.39}_{-0.41}$	$-0.055^{+0.041}_{-0.043}$	$+0.5$
$\langle P_2\rangle_{[0.1,2]}$	$0.03^{+0.14}_{-0.15}$	$0.172^{+0.020}_{-0.021}$	-1.0
$\langle P_2\rangle_{[2,4.3]}$	$0.50^{+0.00}_{-0.07}$	$0.234^{+0.060}_{-0.086}$	**$+2.9$**
$\langle P_2\rangle_{[4.3,8.68]}$	$-0.25^{+0.07}_{-0.08}$	$-0.407^{+0.049}_{-0.037}$	**$+1.7$**
$\langle P_2\rangle_{[1,6]}$	$0.33^{+0.11}_{-0.12}$	$0.084^{+0.060}_{-0.078}$	$+1.8$
$\langle A_{\rm FB}\rangle_{[0.1,2]}$	$-0.02^{+0.13}_{-0.13}$	$-0.136^{+0.051}_{-0.048}$	$+0.8$
$\langle A_{\rm FB}\rangle_{[2,4.3]}$	$-0.20^{+0.08}_{-0.08}$	$-0.081^{+0.055}_{-0.069}$	-1.1
$\langle A_{\rm FB}\rangle_{[4.3,8.68]}$	$0.16^{+0.06}_{-0.05}$	$0.220^{+0.138}_{-0.113}$	-0.5
$\langle A_{\rm FB}\rangle_{[1,6]}$	$-0.17^{+0.06}_{-0.06}$	$-0.035^{+0.037}_{-0.034}$	-2.0

- **P_1**: No substantial deviation (large error bars).
- **$A_{\rm FB}$-P_2**: A slight tendency for a lower value of the second and third bins of $A_{\rm FB}$ is consistent with a $2.9\,\sigma$ ($1.7\,\sigma$) deviation in the second (third) bin of P_2.
- **Zero**: Preference for a slightly higher q^2-value for the zero of $A_{\rm FB}$ (same as the zero of P_2).

Both effects can be accommodated with $\mathcal{C}_7^{\rm NP} < 0$ and/or $\mathcal{C}_9^{\rm NP} < 0$.

Observable	Experiment	SM prediction	Pull
$\langle P_4'\rangle_{[0.1,2]}$	$0.00^{+0.52}_{-0.52}$	$-0.342^{+0.031}_{-0.026}$	$+0.7$
$\langle P_4'\rangle_{[2,4.3]}$	$0.74^{+0.54}_{-0.60}$	$0.569^{+0.073}_{-0.063}$	$+0.3$
$\langle P_4'\rangle_{[4.3,8.68]}$	$1.18^{+0.26}_{-0.32}$	$1.003^{+0.028}_{-0.032}$	$+0.6$
$\langle P_4'\rangle_{[1,6]}$	$0.58^{+0.32}_{-0.36}$	$0.555^{+0.067}_{-0.058}$	$+0.1$
$\langle P_5'\rangle_{[0.1,2]}$	$0.45^{+0.21}_{-0.24}$	$0.533^{+0.033}_{-0.041}$	-0.4
$\langle P_5'\rangle_{[2,4.3]}$	$0.29^{+0.40}_{-0.39}$	$-0.334^{+0.097}_{-0.113}$	$\mathbf{+1.6}$
$\langle P_5'\rangle_{[4.3,8.68]}$	$-0.19^{+0.16}_{-0.16}$	$-0.872^{+0.053}_{-0.041}$	$\mathbf{+4.0}$
$\langle P_5'\rangle_{[1,6]}$	$0.21^{+0.20}_{-0.21}$	$-0.349^{+0.088}_{-0.100}$	$+2.5$
$\langle P_4'\rangle_{[14.18,16]}$	$-0.18^{+0.54}_{-0.70}$	$1.161^{+0.190}_{-0.332}$	-2.1
$\langle P_4'\rangle_{[16,19]}$	$0.70^{+0.44}_{-0.52}$	$1.263^{+0.119}_{-0.248}$	-1.1
$\langle P_5'\rangle_{[14.18,16]}$	$\mathbf{-0.79^{+0.27}_{-0.22}}$	$\mathbf{-0.779^{+0.328}_{-0.363}}$	$+0.0$
$\langle P_5'\rangle_{[16,19]}$	$\mathbf{-0.60^{+0.21}_{-0.18}}$	$\mathbf{-0.601^{+0.282}_{-0.367}}$	$+0.0$

Definition of the anomaly:

- $\mathbf{P_5'}$: There is a striking $4.0\,\sigma$ ($1.6\,\sigma$) deviation in the third (second) bin of P_5'.

  Consistent with large negative contributions in $\mathcal{C}_7^{\rm NP}$ and/or $\mathcal{C}_9^{\rm NP}$.

- $\mathbf{P_4'}$: in agreement with the SM, but within large uncertainties, and it has future potential to determine the sign of $\mathcal{C}_{10}^{\rm NP}$.

- $\mathbf{P_6'}$ and $\mathbf{P_8'}$: show small deviations with respect to the SM, but such effect would require complex phases in $\mathcal{C}_9^{\rm NP}$ and/or $\mathcal{C}_{10}^{\rm NP}$.

Us: $(-0.19-(-0.872))/\sqrt{0.16^2+0.053^2}=4.05$ and **Exp**: $(-0.19-(-0.872+0.053))/\sqrt{0.16^2+0.053^2}=3.73$

Our SM predictions+LHCb data

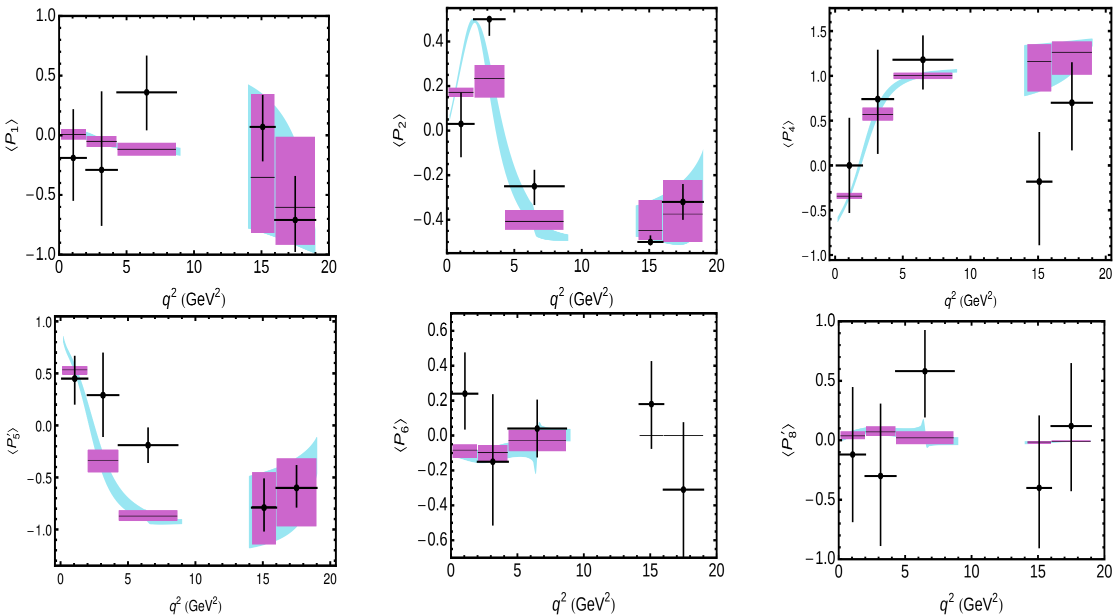

Figure : Experimental measurements and SM predictions for some $B \to K^*\mu^+\mu^-$ observables. The black crosses are the experimental LHCb data. The blue band corresponds to the SM predictions for the differential quantities, whereas the purple boxes indicate the corresponding binned observables.

Description of the analysis

Goal: Determine the Wilson coefficients $\mathcal{C}_{7,9,10}$, $\mathcal{C}'_{7,9,10}$: $\mathcal{C}_i = \mathcal{C}_i^{SM} + \mathcal{C}_i^{NP}$

Standard χ^2 frequentist approach: Asymmetric errors included, estimate theory uncertainties for each set of $\mathcal{C}_i^{NP}$ and all uncertainties are combined in quadrature.

We do three analysis: a) large-recoil data b) large+low-recoil data c) [1-6] bin

Observables:

- $B \to K^*\mu^+\mu^-$: We take observables P_1, P_2, P'_4, P'_5, P'_6, P'_8 and A_{FB} in the following binning:
  - -**large-recoil**: $[0.1, 2], [2, 4.3], [4.3, 8.68]$ GeV^2.
  - -**low recoil**: [14.18,16], [16,19] GeV^2
  - -**wide large-recoil bin**: $[1, 6]$ GeV^2.
- Radiative and dileptonic B decays: $\mathcal{B}(B \to X_s\gamma)_{E_\gamma > 1.6\mathrm{GeV}}$, $\mathcal{B}(B \to X_s\mu^+\mu^-)_{[1,6]}$ and $\mathcal{B}(B_s \to \mu^+\mu^-)$, $A_I(B \to K^*\gamma)$ and the $B \to K^*\gamma$ time-dependent CP asymmetry $S_{K^*\gamma}$

General case all WC free

In conclusion our pattern of [PRD88 (2013) 074002] obtained from an $\mathcal{H}_{eff}$ approach is

$$\mathbf{C_9^{NP}} \sim [-\mathbf{1.6}, -\mathbf{0.9}] > \mathbf{3}\sigma, \quad \mathbf{C_7^{NP}} \sim [-\mathbf{0.05}, -\mathbf{0.01}] \text{ at } \mathbf{2}\sigma, \quad \mathbf{C_9'} \sim \pm\delta\,(\mathbf{SM}) \quad \mathbf{C_{10}}, \mathbf{C'_{7,10}} \sim \pm\epsilon\,(\mathbf{SM})$$

where δ is small and compatible with zero (SM) and ϵ is smaller.

$\Rightarrow$ There is **strong evidence for a $\mathcal{C}_9^{\rm NP} < 0$, preference for $\mathcal{C}_7^{\rm NP} < 0$** and **no clear-cut evidence** for $\mathcal{C}^{\rm NP}_{10,7\prime,9\prime,10\prime} \neq 0$.

A simplified version is $C_9^{NP} = -1.2$ or -1.5 with C_9^{SM} including **all known em corrections**.

Best fit points we find in different scenarios:

Large recoil: $\mathbf{C_9^{NP}} = -\mathbf{1.5}$, $C^{\rm NP}_{7eff} = -0.02$

Large recoil: $\mathbf{C_9^{NP}} = -\mathbf{1.6}$, $C^{\rm NP}_{7eff} = -0.02$, $C^{\rm NP}_{10} > 0$, $\mathbf{C^{NP}_{9\prime}} < \mathbf{0}$, $C^{\rm NP}_{7\prime} > 0$, $C^{\rm NP}_{10\prime} < 0$.

Large+Low: $\mathbf{C_9^{NP}} = -\mathbf{1.2}$, $C^{\rm NP}_{7eff} = -0.03$, $C^{\rm NP}_{10} > 0$, $\mathbf{C^{NP}_{9\prime}} > \mathbf{0}$, $C^{\rm NP}_{7\prime} < 0$, $C^{\rm NP}_{10\prime} < 0$

Branching Ratio of $B \to K^* \mu^+ \mu^-$ and $B \to K \mu^+ \mu^-$

→ BR are strongly dependent on FF choices (for lattice FF see S. Meinel's talk)
→ We use them as cross check. → $B \to K\mu\mu$ provides info on $C_9^{NP} + C_9'$.

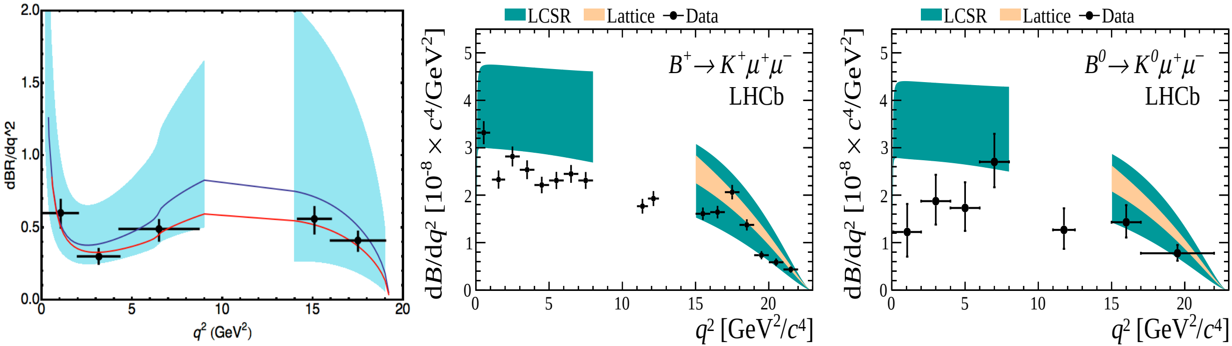

(**left**) $BR(B \to K^*\mu\mu)$: blue curve is SM and red curve corresponds to $C_9^{NP} = -1.5$.

• 3 fb^{-1} data on $B^- \to K^-\mu^+\mu^-$ and $B^0 \to K^0\mu^+\mu^-$ exhibit a similar deficit w.r.t. SM at large-recoil.

• A 2^{nd} **proposed solution** by Altmannshofer-Straub $-C_9^{NP} \sim C_9' \sim 1$ constructed to reproduce the SM is in trouble. At **large-recoil** this 2^{nd} solution is **in tension** with the new 3 fb^{-1} data of **both** modes.

• On the contrary this data is in very good **agreement with our solution** particularly at large but also at low-recoil. We use updated WC, full expressions for the BR including important **quadratic terms**.

[Hofer, Descotes, Mescia, JM, Virto]

Possible explanations of the observed discrepancies in $B \to K^* \mu^+ \mu^-$:

1. Underestimated theory errors: Our plots include all known pieces in QCDF in SM.

   There are three issues that can only be estimated:

   i) Factorizable and non-factorizable power corrections (see J. Virto talk's).
   ii) Charm-loop contributions.
   iii) Quark-hadron duality violations at low-recoil.

   We have verified that the "usual suspects" i) and ii) does not provide a successful explanation of the observed discrepancies at large-recoil. At low-recoil iii) will be important.

2. Experimental issue [statistical Fluctuation (we are still with 1 fb^{-1} dataset),...].

3. New Physics contribution mainly to the Wilson coefficient of the semileptonic operator O_9. This is already discussed and it is the main conclusion of our analysis.

OPTION 1:

Theoretical uncertainties

There are basically two approaches:

$\boxed{\Rightarrow}$ **Soft FF + NLO QCDF** ($O(\alpha_s)$-factorizable+non-factorizable+weak annihilation) [BFS'01,'04]

[Descotes, Matias, Virto]

+ **factorizable and non-factorizable power corrections** [S. Descotes, L. Hofer, J. Matias, J. Virto]

$$F = F^{\rm soft}(\xi_\perp, \xi_\|) + \Delta F^{\alpha_s} + a_F + b_F \frac{q^2}{m_B^2} + c_F \frac{q^4}{m_B^4} \quad \text{and} \quad A_i = A_i^0 + d_F + e_F \frac{q^2}{m_B^2}$$

[Jaeger, Camalich]

$\boxed{\Rightarrow}$ **Naive factorization (full form factors) + non-factorizable QCDF**

(some weak annihilation neglected) [Altmannshoffer, Ball, Barucha, Buras, Straub, Wick]

+ **non-factorizable power corrections** [S. Descotes, L. Hofer, J. Matias, J. Virto]

We have worked out the two options in three different schemes.

Conclusion: **We find that the impact of power corrections is SUBSTANTIALLY smaller than claimed in previous works and far from explaining any anomaly.**

A *third complementary approach* for a future analysis of data for a second round of LHCb data

$\boxed{\Rightarrow}$ **Amplitude analysis** (see Petridis's talk)

- Use symmetries to fix 4 real/imaginary parts of amplitudes to zero.
- Parametrize amplitudes by $A_i = \alpha_i + \beta_i q^2 + \gamma_i / q^2$. How to provide this info to theorists?

The impact of factorizable power corrections is indeed smaller than previous estimates.

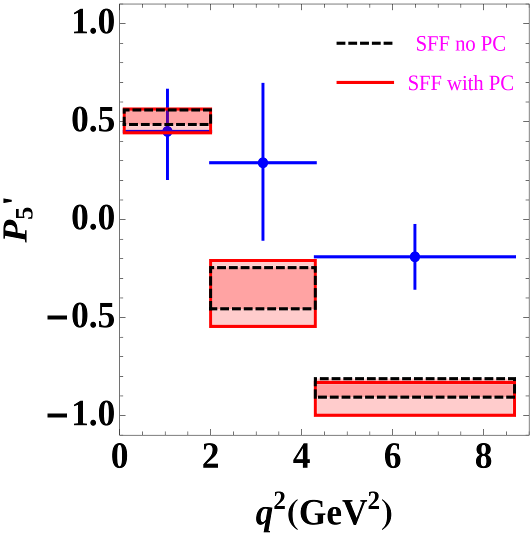

We use KMPW Form Factors.
Similar results using Ball-Zwicky.

Our method: SFF from full FF

I. Fit a_F, b_F, c_F to reproduce exactly full FF

II. Take $\Delta a_F = \Delta b_F = \Delta c_F = \mathcal{O}(\Lambda/m_B) \times F(0)$ corresponding to $> 100\%$ error w.r. to a_F, b_F, c_F.

Main improvements:

- Understand importance of choosing the right scheme to
  - maximize the dependence on known quantities $\xi_{\perp,\|}$
  - minimizes the dependence on unknown ones (correlation between errors of PC).
- Use of all correlations among a_i, b_i, c_i:
  - depend on scheme choice
  - exact relations of FF at $q^2 = 0$.
- In JC approach:
  - two different q^2 dependence for soft FF used at the same time $\xi_\perp(q^2) = \xi_\perp(0)/(1 - \frac{q^2}{m_b^2})^2$ and $\xi_\perp(q^2) = T_1(q^2)$
  - averaging different FF parametrization break correlations.
  - "unlucky" choice of scheme that maximizes error

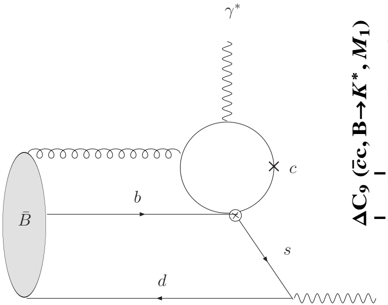

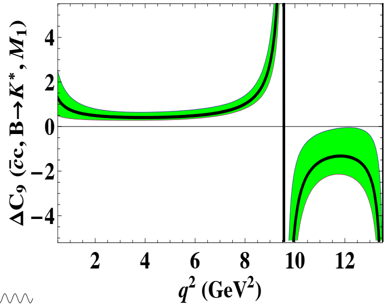

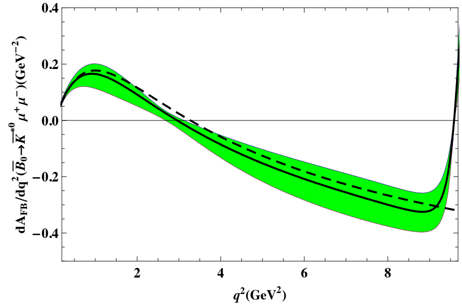

- *Charm loop*: Insertion of 4-quark operators ($\mathcal{O}^c_{1,2}$) or penguin operators ($\mathcal{O}_{3-6}$) are important and influence the extraction of C_9. Perturbative contribution is absorbed in C_9^{eff}. Long distance:
  - Partly cancelled experimentally by removing charmonium resonances.
  - **We followed LCSR computation and prescription** from KMPW to recast the effect inside C_9 as an effective contribution (different for each amplitude). See plots above taken from KMPW.

Result:
  - An increase of charm mass, for instance, from 1.27 to 1.4 GeV shifts C_9^{NP} by $+0.3$ in the third bin, reducing its negative value.
  - On the contrary **we checked explicitly** that this long distance charm contributions obtained by KMPW will tend to slightly **enhance** the negativity of C_9^{NP} $\Rightarrow$ **It increases the anomaly in P_5'**.

- It corresponds to large $\sqrt{q^2} \sim \mathcal{O}(m_b)$ above Ψ' mass, i.e., E_K is around GeV or below.
- Methodology:
  - Operator Product Expansion in $E_K/\sqrt{q^2}$ or $\Lambda_{QCD}/\sqrt{q^2}$
  - Form factors in this region:
    - $\rightarrow$ Extrapolation of LCSR FF above 14 GeV^2 [Bobeth, van Dyk, Hiller]
    - $\rightarrow$ Lattice form factors [Bouchard et al,. S. Meinel et al.]
- **Main problem:**

Existence of $c\bar{c}$ **resonances** observed in this region for the related mode $B^- \rightarrow K^-\mu^+\mu^-$ (clearly seen $\psi(4160)$), but many more expected to be seen from BESS-II data.

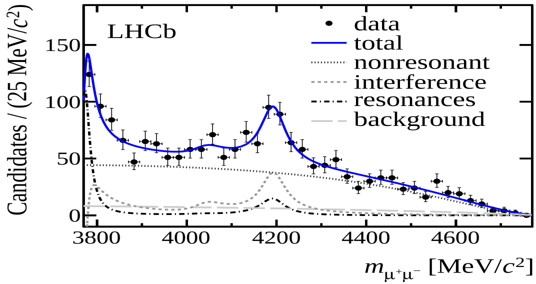

One would expect to observe also a peaking structure at the low-recoil of $B \rightarrow K^*\mu^+\mu^-$

$\Rightarrow$ Quark-hadron duality-violations. How to estimate quark-hadron duality violations:

- First estimate from [Grinstein-Pirjol] combining OPE/HQET gives violation around 5%
- Analysis from [Beylich,Buchalla,Feldmann] estimated to 2%. BUT:
  - Simple toy model estimate based on Shifman's model: OPE+ Δ_2 (oscillating function, exponentially suppressed: duality violating term). Right: simple model based on BES data summing pairs of close resonances, excluding first narrow resonance at $\psi(3770)$ ($q^2 = 14.2$ GeV^2).

Assumption: Neglect interactions between $c\bar{c}$ and $B \to K$ system.

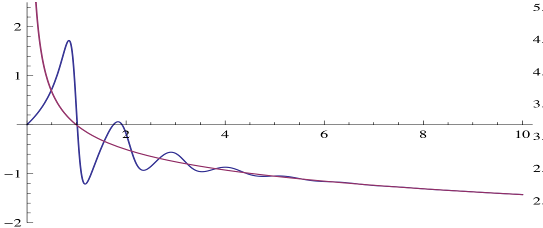

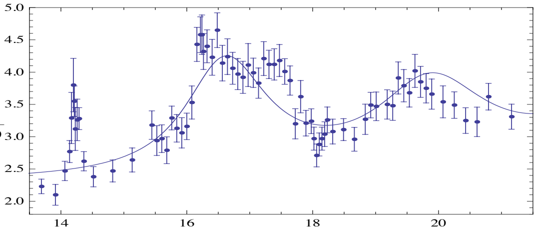

Still open questions:

1. Integrate all bin (starting from 15 and not 14.18 GeV^2 to avoid $\psi(3770)$ problem) and then assign a duality-violation: 2%?, 5%?, 10%?
2. Focus near the endpoint where resonances are exponentially suppressed?
3. Results of bin-by-bin at low-recoil are unclear if no model included.

Interesting experiment by S. Meinel (remove 1st low-recoil bin and repeat the analysis) in a lattice FF analysis of $B \to K^*\mu\mu$ and $B_s \to \phi\mu\mu$ at high-q^2 [hep-ph 1310.3887].

Result:

- C_9^{NP} remained negative, while C_9' became compatible with zero:

$$\mathbf{C_9^{NP} = -1.0 \pm 0.6}, \quad \mathbf{C_9' = 1.2 \pm 1.0} \quad \to \quad \mathbf{C_9^{NP} = -0.9 \pm 0.7}, \quad \mathbf{C_9' = 0.4 \pm 0.7}$$

  in agreement with our pattern.

This might help in removing the second argument in favor of a C_9' positive and large as claimed by AS:

- **large-recoil** has a strong preference for $C_9' < 0$.
- **low-recoil** shows a preference for $C_9' > 0$.

$\Rightarrow$ *It is possible that the reason of the low-recoil preference for $C_9' > 0$ might be a problem (experimental or presence of a resonance or its tail) in the first low recoil bin.*

Don't forget the strange behavior of this first low-recoil bin of P_4'!!!

Suggestion to LHCb: **Move the first low recoil bin to the right (like in $B^- \to K^-\mu^+\mu^-$): at 15 GeV^2 or above**

OPTION 2:

Experimental issue

[Egede, Hurth, JM, Ramon, Reece'10]

The 4-body angular distribution ($m_\ell = 0$, no scalars) exhibits 4 **symmetries**: transformations of the transversity amplitudes (2 phases, 2 rotations) that leaves the **distribution invariant**

Symmetries $\Rightarrow$ the minimal # observables for each scenario, AND how many J_i are independent:

$$n_{obs} = 2n_A - n_S = n_c - n_d$$

Case	n_c Coefficients	n_A Amplitudes	n_S Symmetries	n_{obs} Observables	n_d relations
$m_\ell = 0,\ A_S = 0$	11	6	4	**8**	**3** $\Leftarrow$
$m_\ell = 0$	11	7	5	9	2
$m_\ell > 0,\ A_S = 0$	11	7	4	10	1
$m_\ell > 0$	12	8	4	12	0

$J_{1s} = 3J_{2s}$, $J_{1c} = -J_{2c}$ and a third non-trivial consistency relation:

$$J_{2c} = -2\frac{(2J_{2s}+J_3)\left(4J_4^2+\beta_\ell^2 J_7^2\right)+(2J_{2s}-J_3)\left(\beta_\ell^2 J_5^2+4J_8^2\right)}{16J_{2s}^2-\left(4J_3^2+\beta_\ell^2 J_{6s}^2+4J_9^2\right)} +4\frac{\beta_\ell^2 J_{6s}(J_4J_5+J_7J_8)+J_9(\beta_\ell^2 J_5J_7-4J_4J_8)}{16J_{2s}^2-\left(4J_3^2+\beta_\ell^2 J_{6s}^2+4J_9^2\right)},$$

Identical equation can be written in terms of the $\bar{J}_i$.

This equation can be expressed in terms of P_i and P_i^{CP} observables to get:

$$\bar{P}_2 = +\frac{1}{2\bar{k}_1}\left[(\bar{P}_4'\bar{P}_5' + \delta_1) + \frac{1}{\beta}\sqrt{(-1+\bar{P}_1+\bar{P}_4'^2)(-1-\bar{P}_1+\beta^2\bar{P}_5'^2)+\delta_2+\delta_3\bar{P}_1+\delta_4\bar{P}_1^2}\right]$$

where

$$\bar{P}_i = P_i + P_i^{CP} \qquad \beta = \sqrt{1-4m_\ell^2/s}$$

The sign in front of the square root is taken "+" everywhere by comparison with exact result in SM, at low-recoil both solutions (+ and -) converge. (Plot with $\delta_i \to 0$)

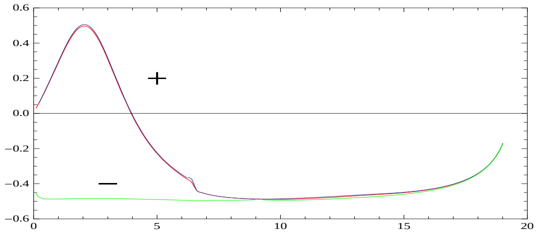

REMARK:

- **This is an exact equation valid for any q^2 (low, large) and obtained from symmetries.**
- **It involves 6 P_i of the basis plus one redundant.**

An identical equation can be written in terms of $\hat{P}_i = P_i - P_i^{CP}$, substituting $\bar{P}_i \to \hat{P}_i$ everywhere. More importantly all terms inside the δ_i are strongly suppressed (by small strong and weak phases):

$$\delta_i \sim \mathcal{O}((\mathrm{Im}A_i)^2, 1-\bar{k}_1) \quad \text{and} \quad \bar{k}_1 = 1 + F_L^{CP}/F_L$$

Hypothesis: No **New Physics in weak phases** entering Wilson coefficients and **not scalars/tensors**. Both hypothesis can be tested, measuring P_i^{CP} and S_1.

To an **excellent approximation** we have:

$$P_2 = \frac{1}{2}\left[P'_4 P'_5 + \frac{1}{\beta}\sqrt{(-1+P_1+P_4'^2)(-1-P_1+\beta^2 P_5'^2)}\right]$$

This equation can be used in *binned form* if:

- Observables are nearly constant inside the bin
- Or the size of the bin is very small.

We correct for this by $\langle P_2 \rangle \to \langle P_2 \rangle + \Delta^{\rm NP}_{\rm exact-relation}$ where $\Delta^{\rm NP}_{\rm exact-relation}$ is order 10^{-2} except for [0.1-2] bin and [1-6] bin.

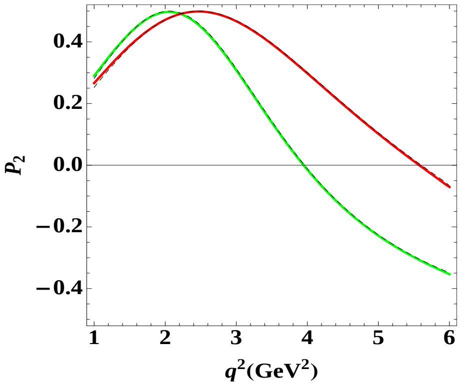

Figure : Green: SM exact, dashed inside approximation, Red: NP $C_9^{NP} = -1.5$ exact, dashed inside approximation

The striking consequence of this equation is that it allows you to use data **to predict** *the* **impact of the anomaly in** P'_5 *in a completely* **different observable***:* P_2

Implication I: **A new bound on P_1**

Imposing that the square root is well defined one finds:

$$P_5'^2 - 1 \leq P_1 \leq 1 - P_4'^2$$

- Indeed this is an exact bound that could be alternatively obtained from

$$|P_4| = |P_4'|/\sqrt{1-P_1} \leq 1 \quad \text{and} \quad |P_5| = |P_5'|/\sqrt{1+P_1} \leq 1$$

$|P_{4,5}| \leq 1$ comes from the geometrical interpretation of those observables in terms of n_i.

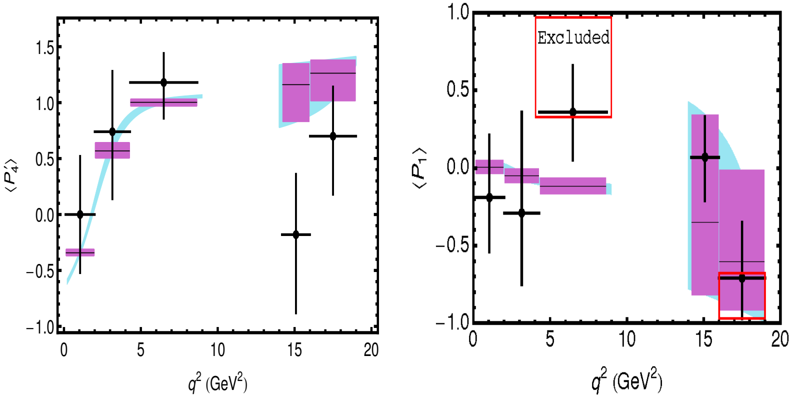

- The new upper bound is very stringent for the [4.3,8.68] bin, cutting most of the space for a positive P_1: $P_1^{[4.3,8.68]} < 0.33$
- The lower bound is particularly relevant for the [16,19] bin of P_1: $P_1^{[16,19]} > -0.68$.

Implication II: **At the position of the zero q_0^2 of P_2 (same as A_{FB}) the following relation holds:**

$$[P_4^2 + P_5^2]|_{q^2=q_0^2} = 1 \quad \text{or} \qquad [P_4'^2 + P_5'^2]|_{q^2=q_0^2} = 1 - \eta(q_0^2)$$

where

$$\eta(q_0^2) = P_1^2 + P_1(P_4'^2 - P_5'^2)|_{q^2=q_0^2}$$

SM Zero of A_{FB}: $q_0^{2SM} = 3.95 \pm 0.38$ (our), 3.90 ± 0.12 (Buras'08), 2.9 ± 0.3 (LO-Khodj.'10) GeV^2

Experimental LHCb data: $q_0^{2LHCb} = 4.9 \pm 0.9$ GeV^2

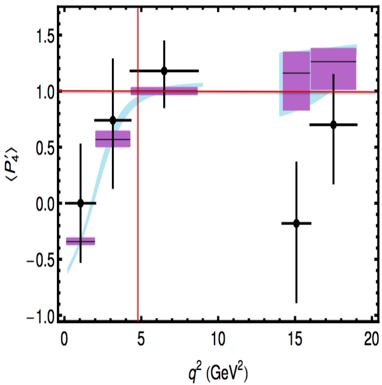

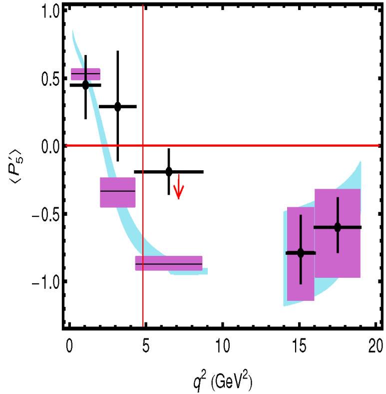

If a future precise measurement of the zero confirms $q_0^{2exp} \sim 4.9$ GeV^2 and $P_4' \sim 1$ and $P_1 \geq 0$ at this point (as present data suggests) THEN

$$P_1(q_0^2) \leq 1 - P_4'^2 \sim 0$$

$$\eta(q_0^2) \sim 0 \textbf{ and } \mathbf{P_5'(q_0^2) \sim 0}$$

(notice that in SM $P_5'(q_0^2) = -0.75$)

A precise measurement of q_0^2 (zero of A_{FB}) outside the SM region would serve as an indirect confirmation of the anomaly

Implication III: **We can establish a new relation between the anomaly bin in P_5' and P_2:**

$$\langle P_2 \rangle = \frac{1}{2}\left[\langle P_4' \rangle \langle P_5' \rangle + \sqrt{(-1 + \langle P_1 \rangle + \langle P_4' \rangle^2)(-1 - \langle P_1 \rangle + \langle P_5' \rangle^2)}\right] + \Delta_{exact}^{bin}$$

where $\Delta_{exact}^{bin} = -0.04$ for NP best fit point at 2nd and 3rd bin, while $\Delta_{exact}^{bin} = -0.01$ for 1 GeV^2 size.

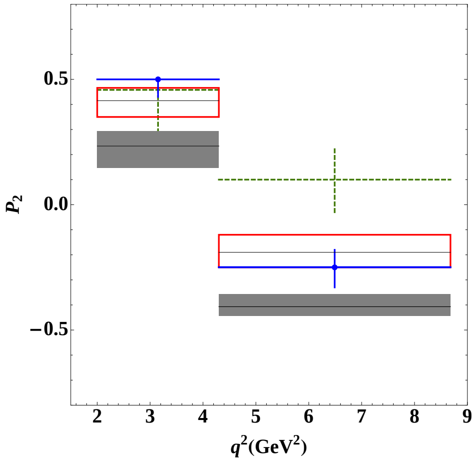

GRAY band: SM prediction.

BLUE cross: Measured value of P_2

RED rectangle: $C_9^{NP} = -1.5$ NP solution.

Green cross is $\langle P_2 \rangle$ obtained from combining data of $\langle P_{4,5}' \rangle$, $\langle P_1 \rangle$, considering asymmetric errors and bound on P_1

- Bin [2,4.3]: LHCb data: $+\mathbf{0.50}^{+0}_{-0.07}$,Relation: $+\mathbf{0.46}^{+0}_{-0.19}$

  0.2σ from relation (green cross) to measured P_2 (blue)

- Bin[4.3,8.68]: LHCb data: $-\mathbf{0.25}^{+0.07}_{-0.08}$, Relation: $+\mathbf{0.10}^{+0.13}_{-0.13}$

  2.4σ from relation (green cross) to measured P_2 (blue),
  1.9σ from relation to NP best fit point (red box),
  3.6σ from relation to SM.

Implication IV:

The first low-recoil bin [14.18,16] can also be tested using this equation

LHCb data on P_2 in this bin gives: $-\mathbf{0.50}^{+0.03}_{-0.00}$

LHCb data on P_4', P_1, P_5' implies that P_2 should be: $+\mathbf{0.50}^{+0}_{-0.27}$ (if $+$) or $-\mathbf{0.50}^{+0.33}_{+0}$ (if -)

- This shows a discrepancy of $\mathbf{3.7}\sigma$ if $+$ solution is taken
- Or agreement if - solution is chosen

However both solutions $+$ and - should give same result at low-recoil

Conclusion: The measurement of this first low recoil bin is probably exhibiting a statistical fluctuation or signaling a problem at low recoil (a large strong phase driven by resonances?)

Implication V:

ALTERNATIVELY Full fit of the angular distribution with a small dataset

Under the assumption of real Wilson coefficients one has

- Free parameters F_L, P_1, $P'_{4,5}$.
- P_2 is a function of the other observables and $P'_{6,8}$ are set to zero.

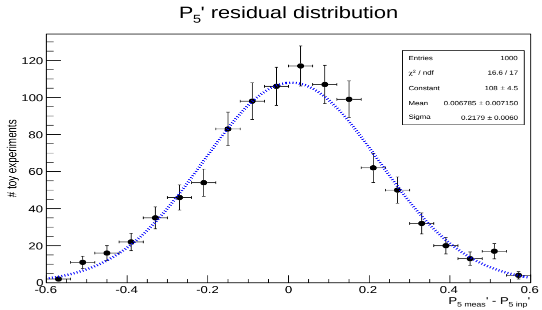

Figure : Residual distribution of P'_5 when fitting with 100 events. The fit of a gaussian distribution is superimosed.

We find testing this fit for values around the measured values: **convergence and unbiased pulls** with as little as 50 events per bin. Gaussian pulls are obtained with only 100 events.

This opens the possibility to perform a full angular fit analysis with small bins in q^2

The main hypothesis (real WC) can be tested measuring P_i^{CP}.

Implication VI: Some of the endpoint symmetries [Zwicky et al] obtained automatically:

$$P_1 = -1 \to P'_5 = 0 = P_2$$

Decision tree

A discrepancy between a measurement of P_2 and the value obtained from data on P_1, $P'_{4,5}$ should be interpreted according to one of the following options:

- At low-q^2 (large-recoil region):

  $\boxed{\text{I}}$ **presence of scalar or tensors**. Improbable given constraints on C_S from $B_s \to \mu^+\mu^-$ (limit on C_S) and strong double suppression m_ℓ^2/q^2 of this term in J_5. Alternatively, one can construct dedicated observables for scalars (S_1 or tensor observables) to test directly this possibility. New Physics

  $\boxed{\text{II}}$ **presence of new Physics contributions in weak phases.** New Physics

  $\boxed{\text{III}}$ **experimental effects** (statistical fluctuation, uncontrolled systematic error, ...)

  II and **III** can be distinguished by studying the pattern of breaking of the equation in all bins:
  - an experimental effect would be most likely localized in particular bins
  - new weak phases would produce a consistent pattern of breaking of the relation and can be observed in A_i^{CP}, P_i^{CP}

- At high-q^2 (low-recoil region): previous possibilities

  $\boxed{\text{IV}}$ An extra possibility is opened: **a new large strong phase** brought by a **resonance**. This case would be recognized by a local breaking of the relation on the bin where the resonance sits.
  - Disentangling II from IV same procedure as before.
  - Disentangling III from IV requires a dedicated experimental analysis of the angles and q^2 in that region allowing for the presence of resonances should be performed

Conclusions

- The analysis of LHCb data on the 4-body angular distribution of $B \to K^*(\to K\pi)\mu^+\mu^-$ using clean $P_i^{(\prime)}$, A_{FB} + radiative observables gives **the pattern**:

$$\mathbf{C_9^{NP}} \sim [-\mathbf{1.6}, -\mathbf{0.9}], \quad \mathbf{C_7^{NP}} \sim [-\mathbf{0.05}, -\mathbf{0.01}], \quad \mathbf{C_9'} \sim \pm\delta \quad \mathbf{C_{10}}, \mathbf{C_{7,10}'} \sim \pm\epsilon$$

  where δ is small and ϵ is smaller. Consistent with new 3 fb^{-1} data on $B \to K\mu\mu$.

- **Large-recoil: 0.1-8.6 GeV^2**: We have shown that the 'usual suspects' does not help in explaining the pattern of deviations in front of a NP explanation:
  - **Charm loops:** The first results from this kind of contributions [Khodjamirian et al.'10] show that they add a positive contribution to C_9, enlarging the size of the discrepancy of data with SM prediction.
  - **Factorizable Power Corrections:** A careful implementation of correlations between PC + the freedom to choose an **appropriate scheme** to define soft FF shows that PC are substantially **smaller** than previously claimed.

  $\Rightarrow$ *Naive statement "It is QCD" is in tension with our detailed analysis.*

- **Low-recoil: 15-19.22 GeV^2**: The difficulty to establish the size of quark-hadron duality violations in this region (2%?, 5%?, ...) complicates the analysis. Different possibilities: i) model resonances, ii) integrate over the whole q^2 region and assign an error,iii) take only the bin near the endpoint...

- We have established a **new connection between the zero of A_{FB} and the anomaly in P_5'** and a full set of consistency tests that experimentalists can use to check the consistency of future data on $B \to K^*\mu^+\mu^-$.

The best possible scenario to move from evidence to discovery:

- P_2:
  - bin [2,4.3] keep the 2.9 σ discrepancy
  - bin [4,3,8.68] should increase the discrepancy w.r.t. the SM. $\Uparrow$
- P_5':
  - bin [2,4.3] should increase the significance of the discrepancy with SM $\Downarrow$
  - bin [4.3,8.68] should decrease the discrepancy possibly reducing a bit the significance. $\Downarrow$

The best strategy would be to split bin [4.3,8.68] into 2 or 3 bins and each one exhibiting a consistent pattern.

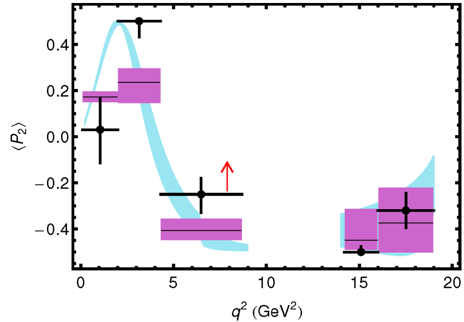

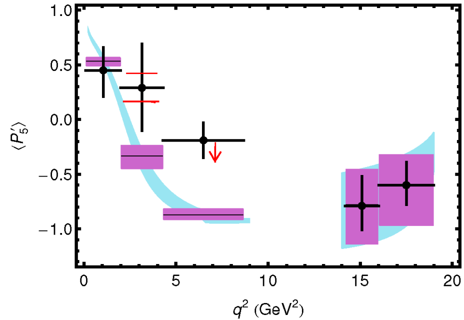

Back-up slides

Relation between J_i and P_j, P'_k observables

The coefficients $\mathbf{J_i}$ of the distribution can be reexpressed now in terms of this basis of clean observables:

Correspondence $\mathbf{J_i} \leftrightarrow \mathbf{P_i^{(\prime)}}$:

BROWN: LO FF-dependent observables (F_L Longitudinal Polarization Fraction of K^*)

RED: LO FF-independent observables at large-recoil (defined from these eqs.)

Here for simplicity ($m_\ell = 0$).
See [J.M'12] for $m_\ell \neq 0$.

$$(\mathbf{J_{2s}} + \bar{\mathbf{J}}_{2s}) = \frac{1}{4}\mathbf{F_T}\frac{d\Gamma + d\bar{\Gamma}}{dq^2} \qquad (\mathbf{J_{2c}} + \bar{\mathbf{J}}_{2c}) = -\mathbf{F_L}\frac{d\Gamma + d\bar{\Gamma}}{dq^2}$$

$$\mathbf{J_3} + \bar{\mathbf{J}}_3 = \frac{1}{2}\mathbf{P_1}\mathbf{F_T}\frac{d\Gamma + d\bar{\Gamma}}{dq^2} \qquad \mathbf{J_3} - \bar{\mathbf{J}}_3 = \frac{1}{2}\mathbf{P_1^{CP}}\mathbf{F_T}\frac{d\Gamma + d\bar{\Gamma}}{dq^2}$$

$$\mathbf{J_{6s}} + \bar{\mathbf{J}}_{6s} = 2\mathbf{P_2}\mathbf{F_T}\frac{d\Gamma + d\bar{\Gamma}}{dq^2} \qquad \mathbf{J_{6s}} - \bar{\mathbf{J}}_{6s} = 2\mathbf{P_2^{CP}}\mathbf{F_T}\frac{d\Gamma + d\bar{\Gamma}}{dq^2}$$

$$\mathbf{J_9} + \bar{\mathbf{J}}_9 = -\mathbf{P_3}\mathbf{F_T}\frac{d\Gamma + d\bar{\Gamma}}{dq^2} \qquad \mathbf{J_9} - \bar{\mathbf{J}}_9 = -\mathbf{P_3^{CP}}\mathbf{F_T}\frac{d\Gamma + d\bar{\Gamma}}{dq^2}$$

$$\mathbf{J_4} + \bar{\mathbf{J}}_4 = \frac{1}{2}\mathbf{P'_4}\sqrt{\mathbf{F_T F_L}}\frac{d\Gamma + d\bar{\Gamma}}{dq^2} \qquad \mathbf{J_4} - \bar{\mathbf{J}}_4 = \frac{1}{2}\mathbf{P_4'^{CP}}\sqrt{\mathbf{F_T F_L}}\frac{d\Gamma + d\bar{\Gamma}}{dq^2}$$

$$\mathbf{J_5} + \bar{\mathbf{J}}_5 = \mathbf{P'_5}\sqrt{\mathbf{F_T F_L}}\frac{d\Gamma + d\bar{\Gamma}}{dq^2} \qquad \mathbf{J_5} - \bar{\mathbf{J}}_5 = \mathbf{P_5'^{CP}}\sqrt{\mathbf{F_T F_L}}\frac{d\Gamma + d\bar{\Gamma}}{dq^2}$$

$$\mathbf{J_7} + \bar{\mathbf{J}}_7 = -\mathbf{P'_6}\sqrt{\mathbf{F_T F_L}}\frac{d\Gamma + d\bar{\Gamma}}{dq^2} \qquad \mathbf{J_7} - \bar{\mathbf{J}}_7 = -\mathbf{P_6'^{CP}}\sqrt{\mathbf{F_T F_L}}\frac{d\Gamma + d\bar{\Gamma}}{dq^2}$$

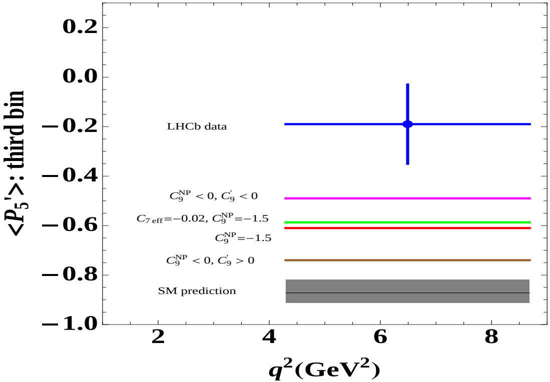

It is not surprising that the second bin in P_2 fits perfectly, while the third bin in P_2 goes on the right direction but does not fit perfectly.

Reason It is very difficult to get excellent agreement with the third bin of P_5' inside a global fit.

— — — (magenta, green, red) $C_9' \leq 0$

— (brown) $C_9' > 0$

- Our large recoil best fit point gives $\langle P_5' \rangle_{[4.3,8.68]} = -0.49$ and reduces tension with data at 1.8σ (from 4σ in SM): $C_9' < 0$ is strongly favored by this bin.
- The best fit point with $C_9^{NP} = -1.5$ gives $\langle P_5' \rangle_{[4.3,8.68]} = -0.61$.
- Any analysis with $C_9' > 0$ provides a much worst disagreement with data in this bin.

Most plausible scenario: Third bin in P_5' will go down (reducing distance with SM) while third bin in P_2 might go up (enlarging distance with SM): *Global picture much more consistent.*

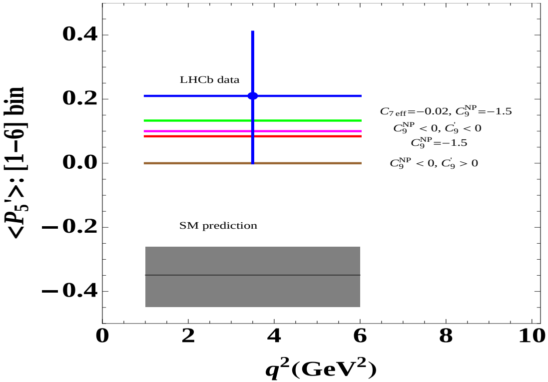

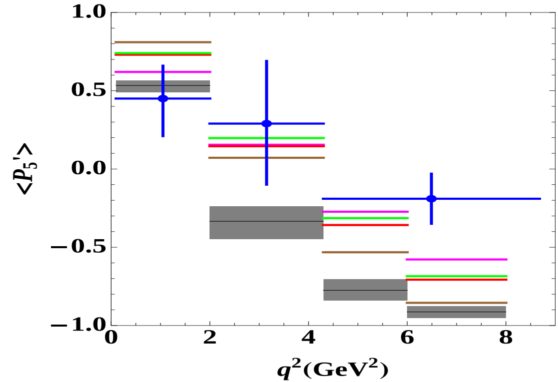

- Our large recoil best fit point gives $\langle P_5' \rangle_{[4.3,8.68]} = -0.49$ and reduces tension with data at 1.8σ (from 4σ in SM): $C_9' < 0$ is strongly favored by this bin.
- The best fit point with $C_9^{NP} = -1.5$ gives $\langle P_5' \rangle_{[4.3,8.68]} = -0.61$.
- Any analysis with $C_9' > 0$ provides a much worst disagreement with data in this bin.

Most plausible scenario: Third bin in P_5' will go down (reducing distance with SM) while third bin in P_2 might go up (enlarging distance with SM): *Global picture much more consistent.*

[Egede, Hurth, JM, Ramon, Reece'10]

If we neglect scalars/tensors the 4-body angular distribution can be written in terms of 3 vectors:

$$\mathbf{n}_{\|} = \begin{pmatrix} A_{\|}^{L} \\ A_{\|}^{R*} \end{pmatrix}, \quad \mathbf{n}_{\perp} = \begin{pmatrix} A_{\perp}^{L} \\ -A_{\perp}^{R*} \end{pmatrix}, \quad \mathbf{n_0} = \begin{pmatrix} A_{0}^{L} \\ A_{0}^{R*} \end{pmatrix}.$$

All the coefficients $\mathbf{J_i}$ can be expressed in terms of the products $\mathbf{n_i^\dagger}\,\mathbf{n_j}$ (example):

$$J_3 = \frac{1}{2}\left(|n_\perp|^2 - |n_\||^2\right), \quad J_4 = \frac{1}{\sqrt{2}}\mathrm{Re}(n_0^\dagger\, n_\|), \quad J_5 = \sqrt{2}\,\mathrm{Re}(n_0^\dagger\, n_\perp), \quad J_9 = -\mathrm{Im}(n_\perp^\dagger\, n_\|)$$

The angular distribution is invariant under a unitary transformation $n_i \to U n_i$

$$n_i^{'} = U n_i = \begin{bmatrix} e^{i\phi_L} & 0 \\ 0 & e^{-i\phi_R} \end{bmatrix} \begin{bmatrix} \cos\theta & -\sin\theta \\ \sin\theta & \cos\theta \end{bmatrix} \begin{bmatrix} \cosh i\tilde{\theta} & -\sinh i\tilde{\theta} \\ -\sinh i\tilde{\theta} & \cosh i\tilde{\theta} \end{bmatrix} n_i\,.$$

U defines the **four symmetries** of the massless angular distribution:

- two global phase transformations (ϕ_L and ϕ_R),
- a rotation θ among the real and imaginary components of the amplitudes independently
- another rotation $\tilde{\theta}$ that mixes real and imaginary components of the transversity amplitudes.

S-wave pollution

[S. Descotes, T. Hurth, JM, J. Virto'13], [J.Matias'12]

- Another possible source of uncertainty is the **S-wave contribution** coming from $B \to K_0^* l^+ l^-$.
  [Becirevic, Tayduganov '13], [Blake et al.'13]
- We assume that both P and S waves are described by q^2-dependent FF $\times$ a Breit-Wigner function.
- The **distinct** angular dependence of the S-wave terms in **folded** distributions allow to disentangle the signal of the P-wave from the S-wave: $P_i^{(\prime)}$ *can be* **disentangled** *from S-wave pollution* [JM'12].

The modified distribution including the **S-wave**:

$$\frac{1}{\Gamma'_{full}} \frac{d^4\Gamma}{dq^2\, d\cos\theta_K\, d\cos\theta_l\, d\phi} = Pdf_{K^*}(1 - \mathbf{F_S}) + \frac{1}{\Gamma'_{full}} \mathbf{W_S}$$

$$\frac{\mathbf{W_S}}{\Gamma'_{full}} = \frac{3}{16\pi} \left[\mathbf{F_S} \sin^2\theta_\ell + \mathbf{A_S} \sin^2\theta_\ell \cos\theta_K + \mathbf{A_S^4} \sin\theta_K \sin 2\theta_\ell \cos\phi \right.$$
$$\left. + \mathbf{A_S^5} \sin\theta_K \sin\theta_\ell \cos\phi + \mathbf{A_S^7} \sin\theta_K \sin\theta_\ell \sin\phi + \mathbf{A_S^8} \sin\theta_K \sin 2\theta_\ell \sin\phi \right]$$

$\Gamma'_{full} = \Gamma'_{K^*} + \Gamma'_S$ and the longitudinal polarization fraction associated to Γ'_S is

$$\mathbf{F_S} = \frac{\Gamma'_S}{\Gamma'_{full}} \quad \text{and} \quad 1 - \mathbf{F_S} = \frac{\Gamma'_{K^*}}{\Gamma'_{full}}$$

We can get **bounds** on the size of the S-wave polluting terms from Cauchy-Schwartz

$$\mathbf{A_S} = 2\sqrt{3}\frac{1}{\Gamma'_{full}}\int \mathrm{Re}\left[(A_0'^{L}A_0^{L*} + A_0'^{R}A_0^{R*})BW_{K_0^*}(m_{K\pi}^2)BW_{K^*}^{\dagger}(m_{K\pi}^2)\right] dm_{K\pi}^2$$

$$|\mathbf{A_S}| \leq 2\sqrt{3}\frac{1}{\Gamma'_{full}} \times \sqrt{[|A_0'^{L}|^2 + |A_0'^{R}|^2][|A_0^L|^2 + |A_0^R|^2]}\,\mathbf{Z} = 2\sqrt{3}\sqrt{\mathbf{F_S(1-F_S)F_L}}\,\mathbf{Z}/\sqrt{\mathbf{XY}}$$

$\mathbf{X}, \mathbf{Y}, \mathbf{Z}$ collect the Breit-Wigner.

[S.Descotes,T, Hurth, JM,J. Virto 1303.5794]

Coefficient	Large recoil ∞ Range	Low recoil ∞ Range	Large Recoil Finite Range	Low Recoil Finite Range
$\lvert A_S\rvert$	0.33	0.25	0.67	0.49
$\lvert A_S^4\rvert$	0.05	0.10	0.11	0.19
$\lvert A_S^5\rvert$	0.11	0.11	0.22	0.23
$\lvert A_S^7\rvert$	0.11	0.19	0.22	0.38
$\lvert A_S^8\rvert$	0.05	0.06	0.11	0.11

Table : Illustrative values of the size of the bounds for the choices of F_S, F_L, P_1 and $\mathbf{F} = \mathbf{Z}/\sqrt{\mathbf{XY}}$

- **Large-recoil**: $F_S \sim 7\%$ (like $B^0 \to J/\psi K^+\pi^-$), $F_L \sim 0.7$ and $P_1 \sim 0$
- **Low-recoil**: $F_S \sim 7\%$, $F_L \sim 0.38$ and $P_1 \sim -0.48$.

This may help in estimating the **systematics** associated to S-wave.

P_1 and P_2 observables function of $A_\perp$ and $A_\parallel$ amplitudes

- **$\mathbf{P_1}$**: Proportional to $|A_\perp|^2 - |A_\parallel|^2$
  - Test the LH structure of SM and/or existence of RH currents that breaks $A_\perp \sim -A_\parallel$
- **$\mathbf{P_2}$**: Proportional to $\mathrm{Re}(A_i A_j)$
  - Zero of P_2 at the same position as the zero of A_{FB}
  - P_2 is the clean version of A_{FB}. Their different normalizations offer different sensitivities.

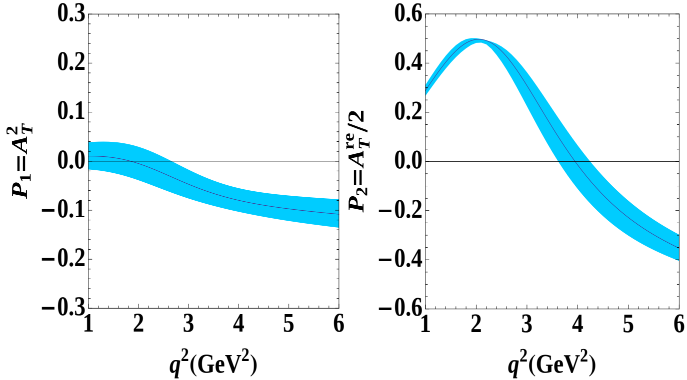

- P_3 and $P'_{6,8}$ are proportional to $\mathrm{Im} A_i A_j$ and small if there are no large phases. All are < 0.1.
- P_i^{CP} are all negligibly small if there is no New Physics in weak phases.

P'_4 and P'_5 observables function of $A_{\perp,\|}$ and also A_0 amplitudes

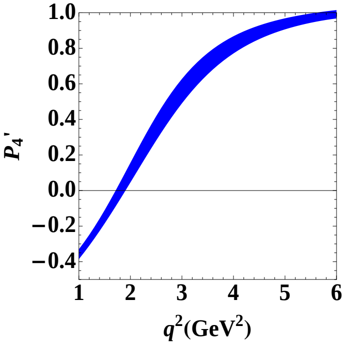

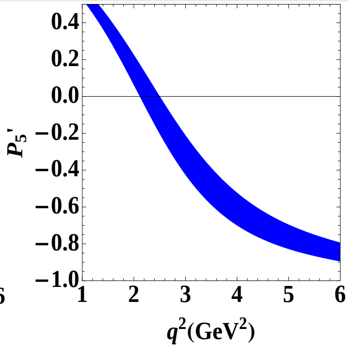

- $\mathbf{P'_{4,5}}$: Proportional to $\mathrm{Re}(A_i A_j)$
- $|P_{4,5}| \leq 1$ but $|P'_{4,5}|$ can be > 1.

In the large-recoil limit

$$A^L_{\perp,\|} \propto \left[\mathcal{C}_9^{\rm eff} - \mathcal{C}_{10} + \frac{2\hat{m}_b}{\hat{s}}\mathcal{C}_7^{\rm eff}\right]\xi_\perp(E_{K^*}) \qquad A^R_{\perp,\|} \propto \left[\mathcal{C}_9^{\rm eff} + \mathcal{C}_{10} + \frac{2\hat{m}_b}{\hat{s}}\mathcal{C}_7^{\rm eff}\right]\xi_\perp(E_{K^*})$$

$$A^L_0 \propto \left[\mathcal{C}_9^{\rm eff} - \mathcal{C}_{10} + 2\hat{m}_b\mathcal{C}_7^{\rm eff}\right]\xi_\|(E_{K^*}) \quad A^R_0 \propto \left[\mathcal{C}_9^{\rm eff} + \mathcal{C}_{10} + 2\hat{m}_b\mathcal{C}_7^{\rm eff}\right]\xi_\|(E_{K^*})$$

• In the SM $C_9^{SM} \sim -C_{10}^{SM}$, this cancellation strongly suppresses $A^R_{\perp,\|}$ above 4 Gev^2: $A^L_{\perp,\|} >> A^R_{\perp,\|}$. This makes $P_4 \to 1$ and $P_5 \to -1$ for $q^2 \to 8$ GeV^2 quite fast BUT the fact that $|A_\|| > |A_\perp|$ and that $P'_4 \propto A_0^{L*}A_\|^L + A_0^R A_\|^{R*}$ and $P'_5 \propto A_0^{L*}A_\perp^L - A_0^R A_\perp^{R*}$ makes less efficient the convergence in the case of P'_5.

• In presence of New Physics affecting only C_9 the cancellation $C_9 \sim -C_{10}$ is less efective, consequently $A^R_{\perp,\|}$ is less suppressed and one should expect to see the effect of $C_9 \neq C_9^{SM}$ in P'_5.